Hindawi
Wireless Communications and Mobile Computing
Volume 2022, Article ID 7268083, 9 pages
https://doi.org/10.1155/2022/7268083

Research Article

Multiobjective Optimization Designs in Downlink NOMA Transmission Systems

Zhe Li

School of Information Engineering, Department of Public Security, Railway Police College, Zhengzhou, China

Correspondence should be addressed to Zhe Li; lizhe@rpc.edu.cn

Received 7 April 2022; Revised 11 May 2022; Accepted 24 May 2022; Published 20 July 2022

Academic Editor: Xingwang Li

To further balance the high-capacity transmission requirement and the scarce spectrum resources status quo, we investigate the joint optimization of energy efficiency (EE) and spectral efficiency (SE) in a downlink multiuser NOMA system. While ensuring the user quality of service (QoS), a power allocation algorithm based on two-layer optimization is proposed by transforming the original multiobjective optimization problem into a univariate problem through the linear weighted sum method. Based on the optimal user power allocation coefficient solution obtained from the inner layer, the outer layer applies the bisection principle to search for the optimal system transmit power according to the uniqueness of the maximum value of pseudo-concave functions. Simulation results show that the proposed algorithm always converges within fewer iterations and can achieve the flexible tradeoff between EE and SE. This is of great significance for improving the energy utilization of actual scenarios with time-varying communication demands.

1. Introduction

The application and popularization of 5G not only accelerates the development of the Internet of Things (IoT) but also promotes the emergence of many new communication services, which brings more strict performance requirements, such as better spectrum efficiency, denser network device access, and ultra-low transmission delay [1–3]. Taking into account the nearly exhausted frequency band resources, relevant scholars and research institutions begin to seek new access technologies to deal with the above problem [4]. Therefore, how to efficiently utilize the limited energy to meet the ever-increasing communication demand becomes a major topic in the current mobile communication field.

Coincidentally, as a prominent wireless radio technique, nonorthogonal multiple access (NOMA) can transmit multiple users' information simultaneously in the same frequency by introducing the power domain dimension, which generates excellent spectral efficiency (SE) [5, 6]. Especially, the key technology determining the performance of NOMA is power multiplexing [7]. Therefore, in the background of the high energy consumption and great demand for data rates in wireless communication system, it desperately needs more efficient power allocation schemes that consider altogether energy efficiency (EE), SE, and quality of service (QoS) to maintain the superiority of NOMA.

Generally, the power allocation in NOMA is mainly discussed from two aspects, i.e., EE and SE. From EE vantage point, a fast convergence algorithm based on the Dinkelbach-Like theory was presented in [8], which contributes to obtain the optimal EE for a multiuser NOMA system. In [9], Z. Ma et al. investigated the problem about jointing user and subcarrier allocation while considering user fairness in a downlink multicarrier (MC) NOMA system. In [6], K. Cumanan et al. studied how the beamforming technology in MISO NOMA systems can better improve the EE. In addition, extensive researches have also been done from the SE aspect of NOMA. For instance, an effective resource schedule strategy is proposed to enhance the SE for a MC-NOMA system in [10]. In [11], a method for jointing optimal beamforming and power allocation all introduced to improve the throughput of the NOMA networks

in multicell. In [12], a power allocation and spectrum sharing technology for the two-slot and secondary NOMA relay network is given to maximize the overall achievable rate of cellular users.

However, the above-related works all consider the single-objective optimization (SOO) with EE or SE. In fact, the system metric often needs to be flexibly adjusted according to actual communication scenes. In some scenes with high real-time demands, the devices often need to quickly respond to the emergency requirements, such as medical care or alert information, which is SE critical [13]. But in other times, the devices can be served just to maintain its basic operation, and which requires optimal EE at this moment. Thus, it is significant to study how improve the energy utilization by weighing EE and SE in the real-time transmission scenarios. In [14], Y. Hei et al. conducted the parameter analysis and simulation verification for the EE-SE tradeoff in DCO-OFDM communication system. In [15], O. Aydin et al. studied the tradeoff about EE-SE in 5G multioperator heterogeneous networks. Additionally, the closed expressions for the relationship between EE and SE in CRN network were derived in [16], which also claimed that EE-SE are not contradictory in CRN networks and can achieve the optimal tradeoff. In NOMA system, the tradeoff about EE and SE for a single-carrier and multiuser network is investigated in [17], but it still adopted the constraint method, which makes EE as the main optimization objective, and SE as a constraint, in which the acquisition of EE's value is more experience-based and less flexible. In [18], the EE-SE tradeoff in a NOMA system with multiuser pairs was studied, and it assumed that there was no interference between user pairs, which indicates that the power allocation is only based on every two users. An energy-efficient resource allocation technique for a hybrid time division multiple access—NOMA system—was proposed in [19], the available time for transmission is divided into several subtime slots, and a subtime slot is allocated to serve a group of users (i.e., cluster). A network network nonorthogonal multiple access (N-NOMA) technique for the uplink coordinated multipoint transmission (CoMP) was applied in [20] to improve the system throughput, and the numerical results are presented to show the accuracy of the analytical results and also demonstrate the superior performance of the proposed N-NOMA scheme.

Based on the above researches, for improving the energy utilization, we consider both EE and SE as primary optimization goals simultaneously in a downlink multiuser NOMA system. By applying the linear weighted sum function method [21], the original multiobjective optimization (MOO) problem is firstly transformed into a SOO problem through a positive weighting factor. While satisfying users' QoSs, we finally propose a dual-layer power allocation algorithm based on bisection searching. The optimal closed-form expressions for power allocation coefficient of all connected users and the optimal system transmit power can be, respectively, obtained in inner and outer layer optimization. Simulation results demonstrate the validity of the proposed algorithm.

2. System Model

In this paper, a downlink NOMA transmission scenario with multiple users is considered in Figure 1, wherein one centrally located base station (BS) serves M single-antenna users simultaneously. The channel coefficient from the BS to the mth user ($1 \le \mathrm{m} \le M$) is represented by $h_m = g_m d^{-\alpha/2}$, where g_{m} denotes the Rayleigh fading, d is the distance between the mth user and the BS, and α is the path-loss exponent. Without loss of generality, we assume that the BS can obtain the instantaneous user channel state information (CSI), and the channel gains of users are sorted as: $0 < |h_1|^2 \le |h_2|^2 \cdots \le |h_M|^2$.

According to the protocol of NOMA, the BS sends a superimposed signal composed of all users' information to each user through the code superposition technology. At the receiving end, the successive interference cancelation (SIC) is adopted to eliminate the inter-user interference. That is, each user first decodes signal of the user whose channel gain is lower than that of its own, and subtracts it from its received signal. Afterwards, it decodes own signal by treating the signal of users with a higher channel gain than itself as interference. Specifically, the mth user first decodes the ith ($i = 1, 2, \cdots, m-1$) user's information and subtracts it from the superimposed signal it receives, and then the information of the jth ($j = m+1, m+2, \cdots, M$) user is regarded as interference.

Consequently, the achievable data rate of the mth user can be written as:

$$R_m = \log_2\left(1 + \frac{a_m P_T |h_m|^2}{P_T |h_m|^2 \sum_{i=m+1}^{M} a_i + \sigma^2}\right), \ \mathrm{m} = 1, \cdots, M, \quad (1)$$

where P_T represents the maximum available transmit power at the BS, and a_m is the ratio of the allocated power of the mth user to P_T.

Furthermore, the sum rate of the system is expressed as:

$$R = \sum_{\mathrm{m}=1}^{M} R_m. \quad (2)$$

Assuming that the system has the unit bandwidth, the SE and EE can be defined as follows [16]:

$$\eta_{SE} = R, \quad (3)$$

$$\eta_{EE} = \frac{R}{P + P_c}, \quad (4)$$

where P_c is the circuit power consumption, and P is the actual consumed transmit power by BS.

3. Problem Formation

According to previous studies on EE and SE for NOMA systems, SE always grows with the increasing of the transmit power of the BS, while EE first increases and then begins to decrease after achieving its maximum value. This means

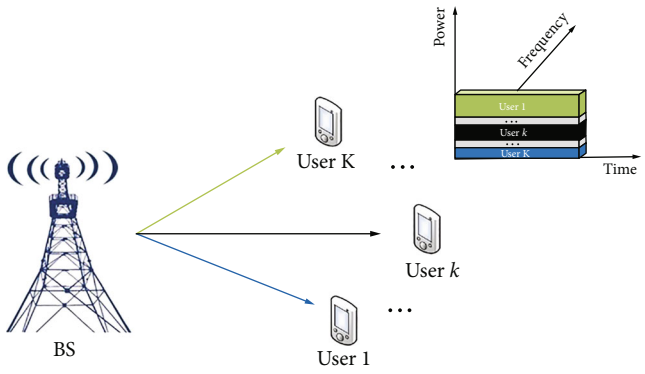

Figure 1: System model.

that EE and SE are contradictory when the BS power is large enough, and also indicates that there is a tradeoff between EE and SE.

In this section, we investigate the joint optimization of EE and SE to achieve a flexible tradeoff between the two. The primordial MOO problem can be formulated as:

$$\mathscr{P}1: \max_{P} \{\eta_{EE}(P), \eta_{SE}(P)\}, \tag{5}$$

where $0 \le P \le P_T$.

Unlike SOO problem, MOO problem can have multiple optimal solutions. For $\mathscr{P}1$, we suppose P^* is the transmit power that enables EE to achieve its maximum value. When $P^* \ge P_T$, $\mathscr{P}1$ only has one solution, i.e., the global optimal solution P_T. When $P^* < P_T$, the objective can be expressed as:

$$\begin{aligned} \mathscr{P}2: &\max_{P} \{\eta_{EE}(P), \eta_{SE}(P)\}, \\ &s.t. P^* \le P \le P_T. \end{aligned} \tag{6a}$$

In order to address $\mathscr{P}2$, we first normalize η_{SE} and η_{EE} to make them additive and comparable, and then, referring to the common conversion method for MOO problems, the weighted sum function is adopted. Afterwards, a new system metric is defined as:

$$W(\lambda_{EE}, \lambda_{SE}) = \omega \cdot \lambda_{EE} + (1-\omega)\lambda_{SE}, \tag{7}$$

where $\lambda_{EE} = \eta_{EE}/\eta_{EE}^{\max}$ and $\lambda_{SE} = \eta_{SE}/\eta_{SE}^{\max}$. $\eta_{EE}^{\max}$ and $\eta_{SE}^{\max}$ are, respectively, the maximum value that EE and SE can achieve within the range of a given BS power. It is evident in (7) that the flexible tradeoff between EE and SE can be realized by adjusting ω ($\omega = \{\omega | 0 \le \omega \le 1\}$), which is a preference factor.

Moreover, substituting (3) and (4) into (7), we get

$$\lambda_{EE-SE} = \left[\omega \frac{1}{\eta_{EE}^{\max}(P + P_c)} + (1-\omega)\frac{1}{\eta_{SE}^{\max}}\right] R. \tag{8}$$

As a result, $\mathscr{P}2$ can be further described as:

$$\mathscr{P}3: \max\ \lambda_{EE-SE}, \tag{9a}$$

$$s.t. R_m \ge R_m^{\min}, 1 \le m \le M, \tag{9b}$$

$$\mathrm{P} \le P_T \text{ and } P = \sum_{m=1}^{M} a_m P_T, \tag{9c}$$

where constraint (9a) denotes the minimum target rate of the mth user, which is required by its QoS and denoted as $R_m^{\min}$ for $1 \le m \le M$. (9b) shows the constraint for maximum transmit power of the BS.

To ensure problem (9) is solvable, the maximum BS transmit power must be large enough to support all users' QoS mentioned in (9a), which further introduces the minimum transmit power constraint. We define $P_{\min}$ as the total minimum transmit power that can just satisfy all users' QoS requirements, and thus, problem (9) is feasible only when $\mathrm{P} \ge P_{\min}$. Therefore, it is important to first establish the feasible range of P, and the derivation of which is discussed as follows.

Denote p_m as the allocated power of the mth user, and the problem of calculating $P_{\min}$ can be described as

$$P_{\min} \triangleq \min_{p_k, 1 \le m \le M} \sum_{m=1}^{M} p_m, \tag{10a}$$

$$s.t. p_m \ge A_m \left(\sum_{i=m+1}^{M} p_i + \frac{\sigma^2}{|h_m|^2}\right), 1 \le m \le M, \tag{10b}$$

where $A_{\mathrm{m}} = 2^{R_m^{\min}} - 1$. And (10b) originates from the minimum target rate constraints in (9b). The solution to problem (10) can be found by using the following theorem.

Theorem 1. *Denoted $\{p_m^{\min}\}_{m=1}^{M}$ as the optimal solution to the objective (10), which is given as*

$$P_m^{\min} = A_m \left(\sum_{i=m+1}^{M} P_i^{\min} + \frac{\sigma^2}{|h_m|^2}\right), 1 \le m \le M. \tag{11}$$

Proof. We prove the theorem according to the contradiction principle. Assuming $\{p_m^*\}_{m=1}^{M}$ is a set of allocated power of all users and also is the optimal solution to problem (10) with at least one constraint in (10b) inactive. More generally, we then set the kth constraint as inactive, i.e.,

$$p_k^* > A_{\mathrm{k}} \left(\sum_{i=k+1}^{K} P_i^{\min} + \frac{\sigma^2}{|h_k|^2}\right). \tag{12}$$

□

We next create $\{P_m^{**}\}_{m=1}^{M}$ as a new set by defining $p_m^{**} = p_m^*$ for $k \ne m$ and setp_k^{**} to the right-hand side (RHS) of (12). By observing the structure of the constraints in (10b), for an arbitrary m, we can find that the RHS of (10b) is a monotonically nondecreasing function of p_i for $1 \le i \le M$. In the result, the setting of p_k^{**}, whose value is less than p_k^{**}, ensures that all the constraints in

(10b) hold for the newly created set $\{P_m^{**}\}_{m=1}^{M}$. But then, we can get $\sum_{m=1}^{M} p_m^{**} < \sum_{M}^{M} M$ with the definition of $\{P_m^{**}\}_{m=1}^{M}$. It obviously contradicts to the assumption that $\{P_m^{**}\}_{m=1}^{M}$ is the optimal solution to problem (10). Therefore, we can conclude that the function (10a) is minimized when all the constraints in (10b) are active. The proof is complete.

Afterwards, when all constraints in (10b) are active, the optimal solution to objective (10), i.e.,$\{P_m^{**}\}_{m=1}^{M}$, can be calculated sequentially in the order $\mathrm{m} = M, M-1, \cdots, 1$, this is because that$P_{\mathrm{m}}^{\min}$ can be calculated by $\{p_{i+1}^{\min}\}_{i=m+1}^{M}$, and $p_M^{\min} = A_M \sigma^2 / |h_m|^2$is determinable. Subsequently, we obtain$P_{\min} = \sum_{m=1}^{K} p_m^{\min}$ and the feasible region of the actual consumed power is $P_{\min} \le P \le P_T$.

4. Proposed Optimal Solutions

It is apparent that $\mathscr{P}3$ is nonconvex, so it is difficult to find the global optimal solution in polynomial time. Therefore, we decompose it into a dual problem, by searching the optimal power allocation in inner layer and optimal available transmit power in outer layer, the final solution of $\mathscr{P}3$ can be obtained.

4.1. Inner Layer: Optimal Power Allocation Scheme. For a given P within the feasible range $P_{\min} \le P \le P_T$, $\mathscr{P}3$ can be regarded as an optimization problem that only includes the power allocation factor a_{m}. Additionally, for any given ω, the part in square brackets on the RHS of (8) is a constant. At this time, problem $\mathscr{P}3$ is equivalent to maximize the overall sum rate R.

Moreover, substituting (1) into (2), R can recast as:

$$\begin{aligned} R = {} & \log_2\left(P_T |h_1|^2 \sum_{i=1}^{M} a_i + \sigma^2\right) \\ & + \sum_{\mathrm{m}=1}^{M-1} \left[\log_2\left(P_T |h_{m+1}|^2 \sum_{i=m+1}^{M} a_i + \sigma^2\right)\right. \\ & \left. - \log_2\left(P_T |h_{\mathrm{m}}|^2 \sum_{i=m+1}^{M} a_i + \sigma^2\right)\right] - \log_2\left(\sigma^2\right). \end{aligned} \tag{13}$$

In order to simplify the notation, we then define:

$$\Gamma_m \triangleq P_T |h_{\mathrm{m}}|^2, 1 \le \mathrm{m} \le M, \tag{14}$$

$$\theta \triangleq \sum_{i=1}^{M} a_i = \frac{P}{P_T}, \tag{15}$$

$$\beta_m \triangleq \sum_{i=m+1}^{M} a_i, 1 \le m \le M-1, \tag{16}$$

$$F_m(\beta_m) \triangleq \log_2\left(\Gamma_{m+1}\beta_m + \sigma^2\right) - \log_2\left(\Gamma_m \beta_m + \sigma^2\right). \tag{17}$$

Based on the above definitions, R can be reformulated as:

$$R = \log_2\left(1 + \Gamma_1 \theta / \sigma^2\right) + \sum_{\mathrm{m}=1}^{M-1} F_m(\beta_m). \tag{18}$$

Here, we further emphasize that $\theta = \{\theta | 0 \le \theta \le 1\}$ is the power consumption factor, which denotes the ratio of the actually utilized power P to the maximum available BS transmit powe rP_T. Therefore, the power allocation of the inner layer is to allocate parameter $\{\mathrm{a}_{\mathrm{m}}^*(\theta)\}_{\mathrm{m}=1}^{M}$ by treating θ as a constant, and its solution is a function of θ. Moreover, it can be easily observed that the first term in (16) is a constant for any given θ, and then the optimization problem for maximizing R is equivalent to:

$$\begin{aligned} \mathscr{P}4 : & \max_{a_m, 1 \le m \le M} \sum_{\mathrm{m}=1}^{M-1} F_m(\beta_m), \\ & s.t.\ R_m \ge R_m^{\min}, \\ & \sum_{m=1}^{M} a_m = \theta, \end{aligned} \tag{19a}$$

where the optimal power allocation coefficient of the mth user, i.e.,$a_{\mathrm{m}}^*(\theta)$, can be obtained by [22]:

$$a_{\mathrm{m}}^*(\theta) = \begin{cases} \dfrac{A_{\mathrm{m}}}{2^{R_{\mathrm{m}}^{\min}}} \left[\theta - \sum_{i=1}^{m-1} a_i^*(\theta) + \dfrac{\sigma^2}{P|h_m|^2}\right], & \mathrm{m} \ne \mathrm{M} \\ \theta - \sum_{i=1}^{m-1} a_i^*(\theta), & \mathrm{m} = \mathrm{M} \end{cases}. \tag{20}$$

4.2. Outer Layer: Optimal Available Transmit Power. In inner layer problem, we have obtained the optimal closed-form solution for the power allocation among users, in which θ is the only variable. Furthermore, in outer layer, $\mathscr{P}3$ can be transformed into a univariate optimization problem about θ.

Based on the optimal power allocation demonstrated in (20), (8) can be rewritten as:

$$\lambda'_{EE-SE}(\theta) = Q(\theta) R(\theta), \tag{21}$$

where

$$Q(\theta) = \frac{\omega}{\eta_{EE}^{\max}(\theta P_T + P_C)} + \frac{1-\omega}{\eta_{SE}^{\max}}, \tag{22}$$

$$R(\theta) = \log_2\left(1 + \Gamma_1 \theta / \sigma^2\right) + \sum_{\mathrm{m}=1}^{M-1} F(\beta_m^*(\theta)), \tag{23}$$

and $\beta_{\mathrm{m}}^*(\theta) = \sum_{i=m+1}^{M} a_i^*(\theta)$, $P = \theta P_T$.

The problem in outer layer can be finally formulated as:

$$\mathscr{P}5: \max_{\theta} \lambda'_{EE-SE}(\theta), \tag{24a}$$

$$\text{s.t.} P_{\min}/P_T \le \theta \le 1.. \tag{24b}$$

In order to obtain the optimal solution of $\mathscr{P}5$, we first introduce the following theorem:

Theorem 2. *$\lambda'_{EE-SE}(\theta)$ is a strict pseudo-concave function with respect to θ.*

Proof. Combining (22) and (23), $\lambda'_{EE-SE}(\theta)$ can be re-expressed as:

$$\lambda'_{EE-SE}(\theta) = \frac{\omega R(\theta)}{\eta_{EE}^{\max}(\theta P_T + P_C)} + \frac{1-\omega}{\eta_{SE}^{\max}} R(\theta), \tag{25}$$

where the convexity of $R(\theta)$ can be firstly verified. It is clear that the first term of $R(\theta)$, i.e., $\log_2(1+\Gamma_1\theta/\sigma^2)$, is a logarithmic function with respect to θ, which indicates that it is strictly concave. Moreover, the convexity of the second term, $F_m(\beta_m^*(\theta))$, can be derived recursively from the convexity of $F_m(\beta_m)$. The first-order derivative of $F_m(\beta_m)$ aboutβ_m is given as:

$$\frac{dF_m(\beta_m)}{d\beta_m} = \frac{(\Gamma_{\mathrm{m}+1} - \Gamma_m)\sigma^2}{\ln 2(\Gamma_{\mathrm{m}+1}\beta_m + \sigma^2)(\Gamma_{\mathrm{m}}\beta_m + \sigma^2)} \ge 0, \tag{26}$$

and the second-order derivative can be further derived as:

$$\frac{d^2F_m(\beta_m)}{d{\beta_m}^2} = \frac{-(\Gamma_{m+1} - \Gamma_m)D\sigma^2}{\ln 2[(\Gamma_{\mathrm{m}+1}\beta_m + \sigma^2)(\Gamma_{\mathrm{m}}\beta_m + \sigma^2)]^2} \le 0, \tag{27}$$

where $D = (\Gamma_{\mathrm{m}+1}\beta_m + \sigma^2)\Gamma_{\mathrm{m}} + (\Gamma_{\mathrm{m}}\beta_m + \sigma^2)\Gamma_{\mathrm{m}+1}$. □

Obviously, the second-order derivative of $F_m(\beta_m)$ is nonpositive, which reveals that $F_m(\beta_m)$ is concave with respect to β_m for $1 < m < M-1$. On this basis, we can further come to the conclusion that $F_{\mathrm{m}}(\beta_m^*(\theta))$ is also concave with respect to θ. This is due to the fact that $\{a_i^*(\theta)\}_{i=1}^{M}$ and $\{\beta_{\mathrm{m}}^*(\theta)\}_{m=1}^{M-1}$ are both affine mappings according to their linear expressions, which preserves the convexity of $F_{\mathrm{m}}(\beta_m^*(\theta))$ about θ. As yet, actually, we have proved that $R(\theta)$ is a strictly concave function with respect to θ, this is because it is the summation about $\log_2(\Gamma_1\theta/\sigma^2+1)$ and $F_{\mathrm{m}}(\beta_m^*(\theta))$, which are all strict concave, and the convexity of functions is preserved by addition operations.

Moreover, for arbitrary ω, $\eta_{EE}^{\max}$, and $\eta_{SE}^{\max}$, both are deterministic quantities. Additionally, $\theta P_T + P_C$ is an affine function of θ. Therefore, since the numerator and denominator of the first term on the RHS of (25) are, respectively, strict concave and affine, it can be easily concluded that the first term of $\lambda'_{EE-SE}(\theta)$ is strict pseudo-concave about θ. Clearly, the second term on the RHS of (25) is also strict concave. Finally, based on the additivity of concave functions, we can declare that $\lambda'_{EE-SE}(\theta)$ is a strict pseudo-concave function about θ. The proof is completed.

For any pseudo-concave function, there is a unique maximizer [20], which guarantees the existence and uniqueness of the global optimal solution of objective (24a), i.e., the root of the equation $d\lambda'_{EE-SE}(\theta)/d\theta = 0$, and the expression for $d\lambda'_{EE-SE}(\theta)/d\theta$ is shown as:

$$\frac{d\lambda'_{EE-SE}(\theta)}{d\theta} = \frac{-P_T\omega}{\eta_{EE}^{\max}(\theta P_T + P_c)^2} R(\theta) + \frac{dR(\theta)}{d\theta} Q(\theta), \tag{28}$$

where

$$\frac{dR(\theta)}{d\theta} = \frac{1}{\ln 2}\left(\frac{\Gamma_M(\mathrm{d}a_M^*(\theta)/d\theta)}{\Gamma_M a_M^*(\theta) + \sigma^2}\right),$$

$$\frac{da_{\mathrm{m}}^*(\theta)}{d\theta} = \begin{cases} \dfrac{A_{\mathrm{m}}}{2^{R_{\mathrm{m}}^{\min}}}\left(1 - \displaystyle\sum_{i=1}^{m-1}\frac{da_i^*(\theta)}{d\theta}\right), & m \ne M \\ 1 - \displaystyle\sum_{i=1}^{M-1}\frac{da_i^*(\theta)}{d\theta}, & m = M \end{cases}. \tag{29}$$

At this time, the outer layer optimization problem is transformed into searching the maximum value of the pseudo-concave function $\lambda'_{EE-SE}(\theta)$, which can turn to the bisection algorithm for help.

4.3. Power Allocation Scheme of Joint Optimization the EE and SE. In this section, we proposed the bisection searching-based power allocation algorithm for the joint optimization of EE and SE, which is shown in Algorithm 1, and the process of it can be described as follows, where t is used to record the number of iterations before the algorithm converges.

At the beginning, the BS calculates the minimum transmit power $P_{\min}$ and then determines whether it is in the feasible range $(P_{\min}/P_T) \le \theta \le 1$. If the condition is satisfied, we can further figure out the root of $\lambda'_{EE-SE}(\theta)$, and the value of $d\lambda'_{EE-SE}(\theta)/d\theta$ with the range $[P_{\min}/P_T, 1]$ can be divided into the following three cases:

Case 1: If $d\lambda'_{EE-SE}(\theta)/d\theta|_{\theta=1} \ge 0$, which indicates that λ'_{EE-SE} keeps increasing in feasible range, and the optimal power consumption factor is $\theta^* = 1$.

Case 2: If $\mathrm{d}\lambda'_{EE-SE}/\mathrm{d}\theta|_{\theta=P_{\min}/P_T} \le 0$, which indicates that λ'_{EE-SE} keeps decreasing in feasible range. At this time, the optimal power consumption factor is $\theta^* = P_{\min}/P_T$.

Case 3: If $\mathrm{d}\lambda'_{EE-SE}/\mathrm{d}\theta|_{\theta=P_{\min}/P_T} > 0$ and $\mathrm{d}\lambda'_{EE-SE}/\mathrm{d}\theta|_{\theta=1} < 0$, which indicates that λ'_{EE-SE} first increases and then decreases. Thus, the optimal power consumption factor is $\theta^* \in [P_{\min}/P_T, 1]$ and can be found by using the bisection searching method.

5. Simulation Results

The validity of Algorithm 1 is verified using computer simulations. We assume that the distance d from all users to

1.**Input**:$P_{\min}$,P_T,t,ε;
2.**Initialization**:$\theta_U = 1$, $\theta_L = P_{\min}/P_T$, $t = 1$, $\varepsilon = 10^{-3}$;
3.Given $\theta_U = 1$, the optimal power allocation coefficient
4.can be obtained by using (20), and then calculate Q_U:
5.$Q_U = d\lambda'_{EE-SE}/d\theta|_{\theta=\theta_U}$;
6. ***if***$Q_u \geq 0$
7. $\theta^* = \theta_U$;
8. ***else***
9. Given $\theta_L = P_{\min}/P_T$, the optimal power allocation
10. can be obtained by using (20), and then calculate Q_L:
11. $Q_L = (d\lambda'_{EE-SE}/d\theta)|_{\theta=\theta_L}$;
12. ***if*** $Q_L \leq 0$
13. $\theta^* = \theta_L$;
14. ***else***
15. $\theta_M = \theta_L + \theta_U/2, Q_M = (d\lambda'_{EE-SE}/d\theta)|_{\theta=\theta_M}$;
16. ***while***$|Q_M| \geq \varepsilon$
17. ***if***$Q_L \cdot Q_M > 0$
18. $\theta_L = \theta_M, Q_L = Q_M$;
19. ***else***
20. $\theta_U = \theta_M, Q_U = Q_M$;
21. ***end***
22. t = t + 1;
23. $\theta_M = \theta_L + \theta_U/2$, $Q_M = (d\lambda'_{EE-SE}/d\theta)|_{\theta=\theta_M}$;
24. ***end while***
25.. $\theta^* = \theta_M$;
26. ***end***
27. ***end***
28.**Output**:$\theta^* P_T$, t.

Algorithm 1: Bisection searching-based power allocation algorithm.

Table 1: Simulation parameters.

Parameters	Characteristic
Number of users	$M = 2, 3, 4$
Noise power	σ^2 = -70dBm
Path-loss exponent	$\alpha = 3$
Maximum available transmit power of the BS	$P_T = 5 \sim 30$dBm
Circuit power consumption	$P_c = 28.30$dBm

the BS is the same and $d = 80$m. Besides, we also suppose that all users have the same QoS requirements, which means that $R_m^{\min} = R^{\min} = 1bps/\text{Hz}$ for $1 \leq m \leq M$. Finally, the settings of other parameters are shown in Table 1. Note that if the maximum available transmit power of the BS cannot support all users' minimum rate constraints, we default that the system does not work.

Figure 2 reveals the EE versus SE with variable P_T, and the variation range of P_T is $5 \sim 30$ dBm. As P_T increases, it can be seen that EE first increases with SE, but when EE reaches its optimal value, EE begins to go down while we continue to increase the P_T, and the system power utilization will decrease. This indicates that EE and SE are contradictory when the available BS power is large enough, and there is a tradeoff between the two.

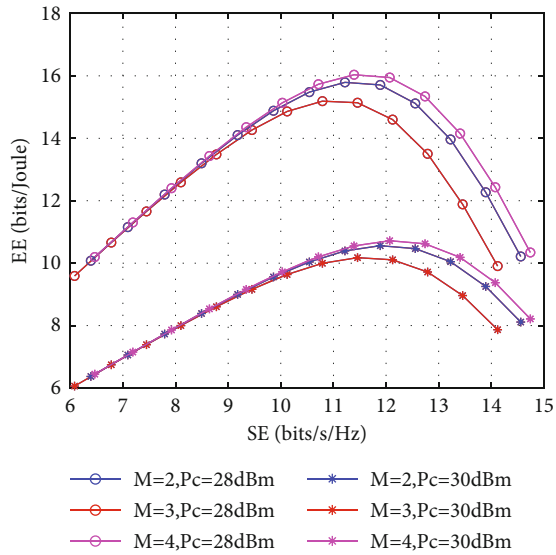

Figure 2: The EE versus SE with different M and P_c ..

Figure 3 shows the EE versus P_T, in which M is set to 2, 3, 4. And "max-SE" means that when the system focuses on maximizing SE, it always applies the full power allocation strategy among users. However, from the EE's point of view, it is obviously not optimal. Because when the power is larger

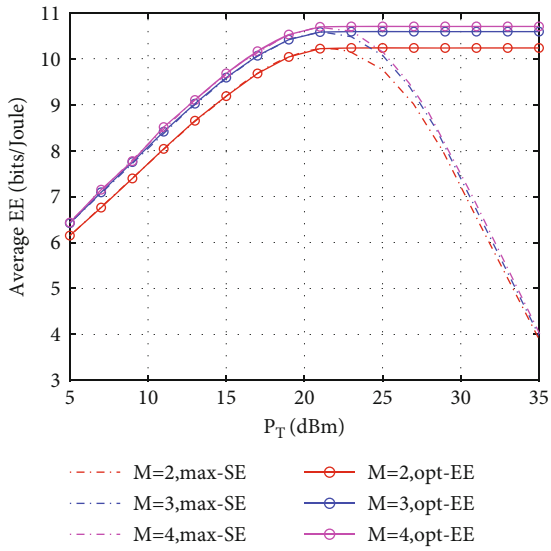

Figure 3: The EE versus P_T of the BS with different M.

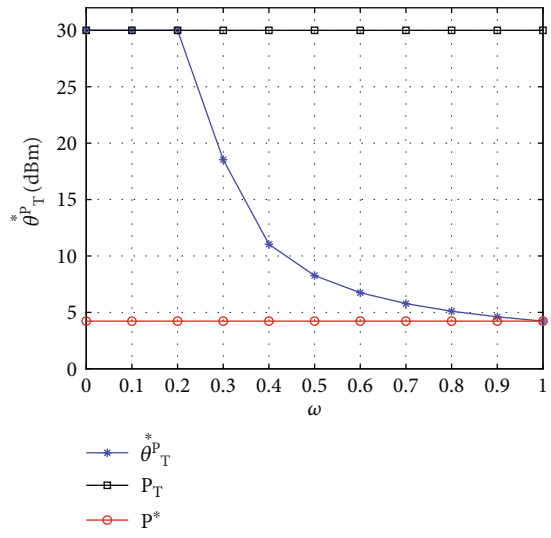

Figure 4: Optimal transmit power $\theta^* P_T$ versus ω.

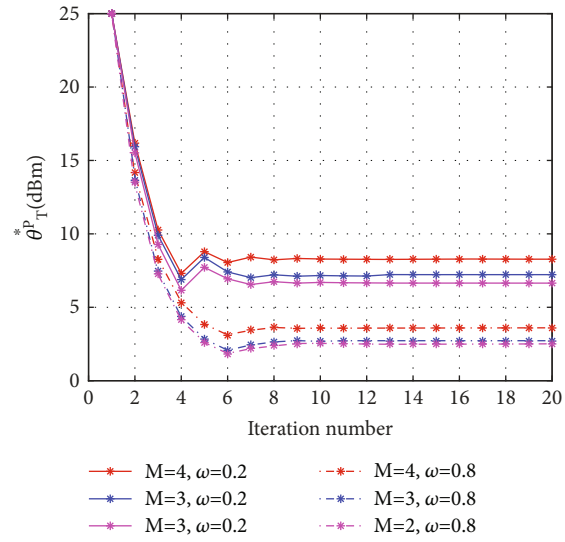

Figure 5: Optimal transmit power $\theta^* P_T$ versus t with different M.

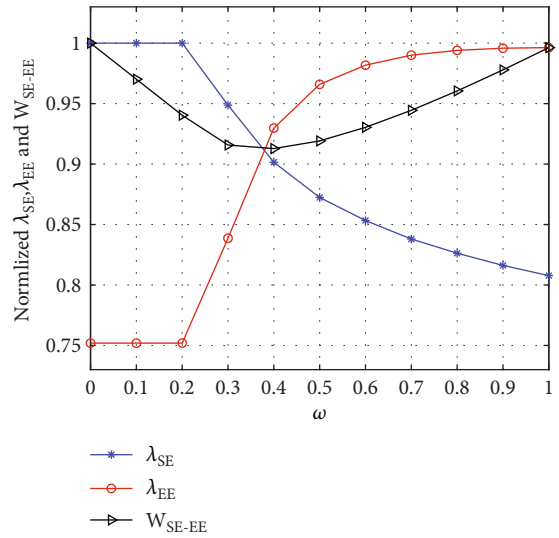

Figure 6: The λ_{EE}, λ_{SE}, and $W(\lambda_{EE}, \lambda_{SE})$ versus ω.

than P^*, EE will increase firstly and then begin to decrease with the increasing of the power. "Opt-EE" means that in the proposed joint optimization algorithm, the system treats EE as an indicator when $\omega = 1$, and the system power can always be maintained at the optimal value that maximizes EE.

Figure 4 depicts the relationship between the optimal transmit power $\theta^* P_T$ and the weighting factor ω. The maximum available transmit power of the BS is set to 30 dBm, i.e., $P_T = 30$dBm, and M is set to 3. It can be seen that as ω increases, $\theta^* P_T$ first remains unchanged at the P_T, and then gradually approaches the P^*. This is because when ω is smaller, the system metric is equivalent to SE, and BS uses as much transmit power as possible to maximize the SE. With the increasing of ω, the system metric gradually transforms to be EE. Therefore, $\theta^* P_T$ gradually approaches P^* that maximizes EE.

Figure 5 reveals $\theta^* \mathrm{P}_T$ versus t with different M in the proposed joint optimization algorithm, where P_T is set to 25 dBm. It can be firstly observed that the actual consumed power grows with the increasing of M. This is because the BS needs more power to provide guaranteeing for the increased users' QoS, but actually, the computational complexity is not significantly enhanced. Because the proposed joint algorithm can always achieve convergence around 7 iterations. More importantly, we can find that the value of $\theta^* P_T$ with $\omega = 0.8$ is obviously smaller than that $\omega = 0.2$. This is due to that the main system metric is the SE, and at this time, the BS always tends to use all power to maximize the system capacity. Oppositely, the main system metric is EE when $\omega = 0.8$, the system always tries to keep the EE at the optimal value, and the value is always less than the power value required to maximize the SE.

Figure 6 investigates the λ_{EE} and λ_{SE}, and the joint objective function $W(\lambda_{EE}, \lambda_{SE})$varying with ω. It can be seen that EE gradually increases with ω, while the SE gradually goes down. However, when the value of ω is close to zero, both EE and SE remain unchanged, which is in consistent with the trend of $\theta^* P_T$ demonstrated in Figure 3. In particular, when $\omega = 0$, the maximum SE can be achieved, and the EE reaches the optimal value when $\omega = 1$.

6. Conclusion

In order to better maintain the system performance and reduce energy consumption, we study the joint optimization of EE and SE in a downlink NOMA system in this paper. We first define a new system performance measurement indicator and then transform the original MOO problem into a SOO problem. Under the condition that guarantees users' QoSs, a two-layer bisection searching-based power allocation algorithm is presented finally. Simulation results verify that the proposed power allocation scheme can achieve the opportune tradeoff between EE and SE by flexibly adjusting the weighting factor in the given indicator function from zero to 1. The method is universal and suitable for improving the energy utilization of actual scenarios with time-varying communication demands.

Data Availability

The data used to support the findings of this study are currently under embargo while the research findings are commercialized. Requests for data, 12 months after publication of this article, will be considered by the corresponding author.

Conflicts of Interest

The author declares that he has no conflicts of interest.

References

[1] X. Fang, W. Feng, T. Wei, Y. Chen, N. Ge, and C. X. Wang, "5G embraces satellites for 6G ubiquitous IoT: basic models for integrated satellite terrestrial networks," *IEEE Internet of Things Journal*, vol. 8, no. 18, pp. 14399–14417.

[2] K. Ali, H. X. Nguyen, Q. T. Vien et al., "Review and implementation of resilient public safety networks: 5G, IoT, and emerging technologies," *IEEE Network*, vol. 35, no. 2, pp. 18–25, 2021.

[3] X. Li, Y. Zheng, W. U. Khan et al., "Physical layer security of cognitive ambient backscatter communications for green Internet-of-Things," *IEEE Transactions on Green Communications and Networking*, vol. 5, no. 3, pp. 1066–1076, 2021.

[4] A. Zappone and E. Jorswieck, "Energy effificiency in wireless networks via fractional programming theory," *Foundations and Trends in Communication and Information Theory*, vol. 11, pp. 185–396, 2014.

[5] X. Li, M. Huang, Y. Liu, V. G. Menon, A. Paul, and Z. Ding, "I/Q imbalance aware nonlinear wireless-powered relaying of B5G networks: security and reliability analysis," *IEEE Transactions on Network Science and Engineering*, vol. 8, no. 4, pp. 2995–3008, 2021.

[6] M. Shirvanimoghaddam, M. Dohler, and S. J. Johnson, "Massive non-orthogonal multiple access for cellular IoT: potentials and limitations," *IEEE Communications Magazine*, vol. 55, no. 9, pp. 55–61, 2017.

[7] Y. Liu, X. Li, F. R. Yu, H. Ji, H. Zhang, and V. C. M. Leung, "Grouping and cooperating among access points in user-centric ultra-dense networks with non-orthogonal multiple access," *IEEE Journal on Selected Areas in Communications*, vol. 35, no. 10, pp. 2295–2311, 2017.

[8] H. Wang, Z. Zhang, and X. Chen, "Energy-efficient power allocation for non-orthogonal multiple access with imperfect successive interference cancellation," in *International Conference on Wireless Communications and Signal Processing (WCSP)*, pp. 1–6, Nanjing, 2017.

[9] A. J. Muhammed, Z. Ma, P. D. Diamantoulakis, L. Li, and G. K. Karagiannidis, "Energy-efficient resource allocation in multi-carrier NOMA systems with fairness," *IEEE Transactions on Communications*, vol. 67, no. 12, pp. 8639–8654, 2019.

[10] Z. Zhu, N. Wang, W. Hao, Z. Wang, and I. Lee, "Robust beamforming designs in secure MIMO SWIPT IoT networks with a nonlinear channel model," *IEEE Internet of Things Journal (Accepted)*, vol. 8, no. 3, pp. 1702–1715.

[11] J. Cui, Y. Liu, Z. Ding, P. Fan, and A. Nallanathan, "QoE-based resource allocation for multi-cell NOMA networks," *IEEE Transactions on Wireless Communications*, vol. 17, no. 9, pp. 6160–6176, 2018.

[12] X. Sun, N. Yang, S. Yan et al., "Joint beamforming and power allocation in downlink NOMA multiuser MIMO networks," *IEEE Transactions on Wireless Communications*, vol. 17, no. 8, pp. 5367–5381, 2018.

[13] B. Chen, Y. Chen, Y. Cao, N. Zhao, and Z. Ding, "A novel spectrum sharing scheme assisted by secondary NOMA relay," *IEEE Wireless Communications Letters*, vol. 7, no. 5, pp. 732–735, 2018.

[14] Y. Hei, Y. Kou, G. Shi, W. Li, and H. Gu, "Energy-spectral efficiency tradeoff in DCO-OFDM visible light communication system," *IEEE Transactions on Vehicular Technology*, vol. 68, no. 10, pp. 9872–9882, 2019.

[15] O. Aydin, E. A. Jorswieck, D. Aziz, and A. Zappone, "Energy-spectral efficiency tradeoffs in 5G multi-operator networks with heterogeneous constraints," *IEEE Transactions on Wireless Communications*, vol. 16, no. 9, pp. 5869–5881, 2017.

[16] W. Zhang, C. Wang, D. Chen, and H. Xiong, "Energy–spectral efficiency tradeoff in cognitive radio networks," *IEEE Transactions on Vehicular Technology*, vol. 65, no. 4, pp. 2208–2218, 2016.

[17] Q. Liu, F. Tan, T. Lv, and H. Gao, "Energy efficiency and spectral-efficiency tradeoff in downlink NOMA systems," in *IEEE International Conference on Comm. Workshops (ICC Workshops)*, pp. 247–252, Paris, 2017.

[18] S. Cetinkaya and H. Arslan, "Energy and spectral efficiency tradeoff in NOMA: multi-objective evolutionary spproaches," in *2020 IEEE International Conference on Communications Workshops (ICC Workshops)*, pp. 1–6, Dublin, Ireland, 2020.

[19] X. Wei, H. M. Al-Obiedollah, K. Cumanan, Z. Ding, and O. A. Dobre, *Energy Efficiency Maximization for Hybrid TDMA-NOMA System with Opportunistic Time Assignment*, IEEE Transactions on Vehicular Technology, 2022.

[20] Y. Sun, Z. Ding, X. Dai, and O. A. Dobre, "On the performance of network NOMA in uplink CoMP systems: a stochastic

geometry approach," *IEEE Transactions on Communications*, vol. 67, no. 7, pp. 5084–5098, 2019.

[21] O. Amin, E. Bedeer, M. H. Ahmed, and O. A. Dobre, "Energy efficiency-spectral efficiency tradeoff: a multiobjective optimization approach," *IEEE Transactions on Vehicular Technology*, vol. 65, no. 4, pp. 1975–1981, 2016.

[22] Y. Zhang, H. Wang, T. Zheng, and Q. Yang, "Energy-efficient transmission design in non-orthogonal multiple access," *IEEE Transactions on Vehicular Technology*, vol. 66, no. 3, pp. 2852–2857, 2017.